

Fluoride Ion Sensing by an Anion- π Interaction

Samit Guha and Sourav Saha*

Department of Chemistry and Biochemistry, Florida State University, 95 Chieftan Way,
Tallahassee, Florida 32306, United States

Received August 16, 2010; E-mail: saha@chem.fsu.edu

Abstract: We report the discovery of a supramolecular interaction (anion- π and charge/electron transfer, CT/ET) involving fluoride ion and π -electron deficient colorless naphthalene diimide (NDI) receptors. Strong electronic interactions between lone-pair electrons of F^- ion and π^* -orbitals of the NDI unit lead to an unprecedented $F^- \rightarrow$ NDI ET event, which produces an orange colored $NDI^{\cdot-}$ radical anion. Further reduction of $NDI^{\cdot-}$ by another F^- ion produces a pink colored NDI^{2-} dianion, rendering NDI a colorimetric F^- sensor. Preorganization of two NDI units in overlapping positions using folded linkers improves their selectivity and sensitivity for the F^- ion significantly, allowing F^- detection at nM concentration in 85:15 DMSO/ H_2O solutions.

The recent discovery of anion- π interaction¹ – a noncovalent interaction between an anion and an electron deficient organic π -system with a strong positive quadrupole moment – has added new dimensions to recognition, sensing,² and transmembrane passage³ of anions. Myriads of anions play critical roles in chemical and biological processes, demanding continuous research in the field of anion recognition.⁴ Dunbar et al.^{2b} recently reported chromogenic anion- π and charge transfer interactions involving halides ($Cl^- > Br^- > I^-$) and electron deficient aromatic rings in organic solvents.

Herein, we present an unprecedented example of chromogenic anion- π and CT interactions involving the F^- ion and π -electron deficient colorless NDI receptors.^{3,5} A plethora of experimental evidence, supported by computational models, indicate that (Figure 1) NDI/F^- interactions facilitate an unprecedented $F^- \rightarrow$ NDI electron transfer (ET) event, which generates an orange $NDI^{\cdot-}$ radical anion. Excess amounts of F^- chemically reduces $NDI^{\cdot-}$ further to a pink NDI^{2-} dianion. Thus, NDI/F^- interactions and ET events produce a two-step optical response, offering a new strategy for toxic F^- ion sensing.

A fluoride deficiency causes osteoporosis and poor dental health.⁶ Overexposure to F^- is blamed for fluorosis and osteosarcoma.⁷ The EPA-recommended F^- level in drinking water is 1 ppm, and over 2 ppm is considered a health-risk.⁸ The low level of F^- tolerance demands for a selective and sensitive F^- sensor. Gabbai and others developed borane, lanthanide, and other Lewis acid based efficient, albeit disposable, F^- sensors.⁹ Conventional hydrogen bonded F^- receptors have also been reported.¹⁰ Because of the nonchromogenic nature of most $Y-H \cdots X^-$ interactions, H-bonded receptors¹⁰ rely on either adjacent chromophore units or deprotonation followed by electron delocalization to display a colorimetric response. Therefore, they cannot differentiate F^- from other strongly basic anions, such as AcO^- and $H_2PO_4^-$.^{10c} In contrast, the selectivity and reusability of NDI-based F^- sensors that exploit reversible anion- π and CT/ET interactions distinguish them from the existing F^- sensors.

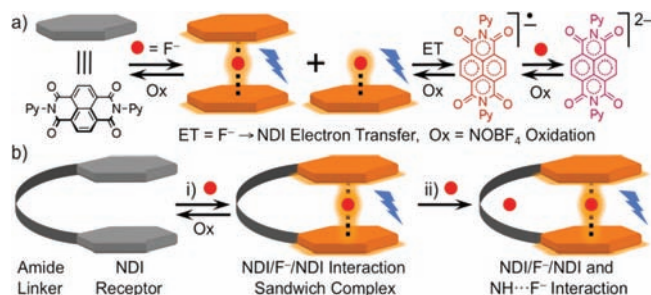


Figure 1. Graphical illustrations of (a) anion- π and CT interactions between F^- and NDI receptor, generating fluorochromogenic response via $F^- \rightarrow$ NDI ET event, (b) stepwise F^- recognition by preorganized receptors (PR) through (i) π -anion- π and (ii) H-bonding interactions.

Iverson and others demonstrated that CT and π - π -stacking interactions between a colorless NDI unit and electron rich aromatic rings produce colored donor-acceptor CT complexes.⁵ We envisioned that NDI units could also bind with appropriate anions through anion- π interactions and report the binding event by generating optical signals on account of anion- \rightarrow NDI CT interactions (Figure 1). To test our hypothesis, we surveyed interactions of NDI receptors with F^- , Cl^- , Br^- , I^- , NO_2^- , NO_3^- , N_3^- , PF_6^- , AcO^- , and $H_2PO_4^-$ anions as tetra-*n*-butylammonium (TBA) salts.

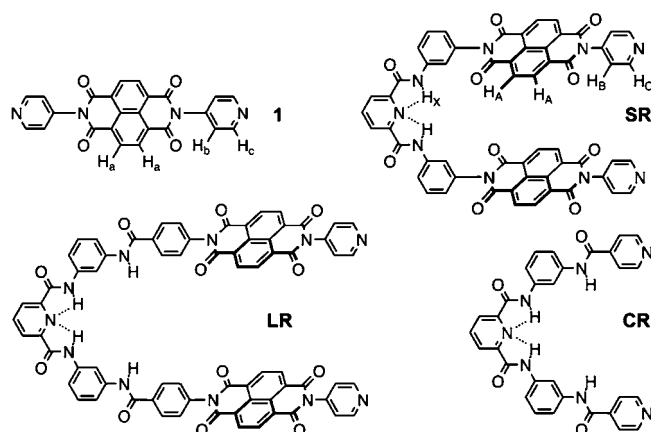


Figure 2. Molecular structures of receptors 1, SR, LR, and CR.

We further postulated that preorganization of two overlapping NDI units by connecting them with folded linkers¹¹ should improve the anion binding affinity, selectivity, and sensitivity. To investigate the effect of preorganization we designed and synthesized (Supporting Information (SI), Scheme S1) NDI receptor 1, a short receptor (SR) containing a bisamide linker connecting two NDI units, a long receptor (LR) containing a tetraamide linker between two NDI units, and a control tetraamide receptor (CR) carrying no NDI unit (Figure 2). Bifurcated intramolecular H-bonds involving

the pivotal pyridine N atom and adjacent amide protons should render the bis- and tetraamide linkers folded conformations that bring two ends of receptor molecules into close proximity.¹¹ Hartree–Fock global energy minimization shows that while the short linker in **SR** brings two NDI units into a parallel overlapping orientation, the longer linker in **LR** projects two NDI units at an angle (SI, Figure S1). In addition to properly orienting NDI units, amide linkers of **SR** and **LR** provide additional anion binding sites in their cavities via H-bonding interaction.

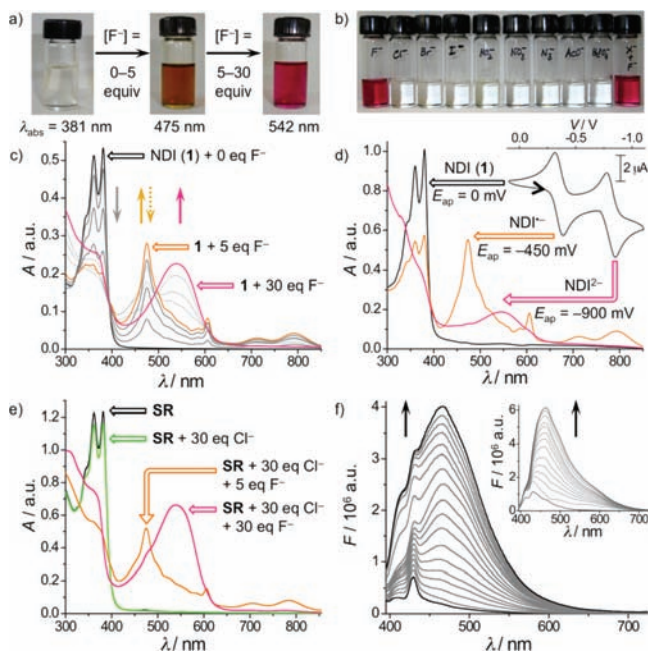


Figure 3. Colorimetric changes of **1** (a) from colorless (no F^-) to orange (0–5 equiv of F^-) to pink (5–30 equiv of F^-) and (b) by other anions (30 equiv) in DMSO. (c) UV/Vis titration of **1** ($10 \mu\text{M}/\text{DMSO}$) with F^- and (d) spectroscopic changes of **1** (0.5 mM in $0.1 \text{ M TBAPF}_6/\text{DMF}$) upon direct electrochemical reduction in the absence of F^- . Black trace: neutral NDI **1** ($E_{\text{ap}} = 0 \text{ mV}$); orange trace: NDI^- ($E_{\text{ap}} = -450 \text{ mV}$); and pink trace: NDI^{2-} ($E_{\text{ap}} = -900 \text{ mV}$). Inset: cyclic voltammogram of **1** (vs Ag/AgCl in $0.1 \text{ M TBAPF}_6/\text{DMF}$) in the absence of F^- . (e) Optical response of **SR** to F^- (orange and pink) in the presence of excess Cl^- but no change only with Cl^- (green vs black). (f) Fluorescence amplifications of **SR** ($1 \text{ nM}/\text{DMSO}$); inset: **1** ($10 \mu\text{M}/\text{DMSO}$) by F^- ion (0–30 equiv F^- , $\lambda_{\text{excitation}} = 381 \text{ nm}$).

The first indication of selective F^- ion sensing by **1**, **SR**, and **LR** came from visible color changes (Figure 3). While Cl^- , Br^- , I^- , NO_2^- , NO_3^- , N_3^- , AcO^- , and H_2PO_4^- even at 30 equiv did not affect the colorless solutions of NDI-based receptors, titrations with F^- in aqueous DMSO, DMF, DMAc, MeCN, Me_2CO , and THF, containing up to 15% of H_2O , immediately changed the color in two steps (Figure 3a,b). At first, the colorless NDI solutions turned orange at lower F^- equivalents (≤ 5 equiv) and then turned pink at higher F^- equivalents (> 5 equiv). NDI-free **CR** did not change color in response to any anion.

ESI-MS confirmed (SI, Figure S2) the formation of $[\mathbf{1}\cdot\text{F}^-]$, $[\mathbf{1}\cdot\text{F}^-\cdot\mathbf{1}]$, $[\mathbf{SR}\cdot\text{F}^-]$, and $[\mathbf{LR}\cdot\text{F}^-]$ complexes by revealing the corresponding peaks at m/z 439.06, 859.15, 1018.28, and 1256.27, respectively, as well as signals associated with **1**, **1**·**1** dimer, **SR**, and **LR** at m/z 420.23, 840.23, 999.25, and 1237.29, respectively, at F^- ion concentrations up to 1 equiv. At 2 equiv of F^- $[\mathbf{SR}\cdot 2\text{F}^-]$ and $[\mathbf{LR}\cdot 2\text{F}^-]$ complexes were found at m/z 518.40 and 637.70, respectively.

UV/Vis titration experiments were conducted to quantify F^- -induced colorimetric transitions of NDI receptors. Receptors **1**, **SR**,

and **LR** display characteristic NDI absorption peaks at 343, 361, and 381 nm. Titration of **1** with 0–5 equiv of F^- gradually bleached NDI absorption peaks and concurrently produced new peaks at 475, 605, 711, and 791 nm, establishing a clear isosbestic point at 394 nm (Figure 3c), as the solution turned orange. The absorption spectrum of orange species generated by F^- (Figure 3c) matches exactly with that of an electrochemically generated NDI^- radical anion (-450 mV vs Ag/AgCl in DMF) produced in the absence of F^- (Figure 3d; orange trace). Manifestations of identical spectroscopic changes with the same isosbestic point (394 nm) during F^- titration (Figure 3c) and during spectroelectrochemical (SEC) analysis of **1** in the absence of F^- (SI, Figure S3a) strongly suggest that the $F^- \rightarrow \text{NDI}$ ET event takes place in the NDI/F^- complex. A nucleophilic attack of F^- on NDI forming a covalent C–F bond should have produced spectroscopic transitions different from SEC. The EPR spectrum (SI, Figure S4) of the F^- -induced orange solution of **1** further confirms the formation of a delocalized NDI^- radical anion ($g = 2.0030$). These results indicate that at first F^- binds with NDI through anion– π and CT interactions that facilitate $F^- \rightarrow \text{NDI}$ electron transfer and generate NDI^- (Figure 1a).

As the solution of **1** turned from orange to pink during the titration with 5–30 equiv of the F^- ion, NDI^- absorption peaks gradually disappeared concomitantly with the emergence of a broad absorption band at 542 nm. This transition at higher F^- equivalents can be attributed to one of the following possibilities: (a) NDI^- is further reduced to NDI^{2-} dianion by another F^- ($E_{1/2} = -2.87 \text{ V}$) or (b) NDI^- is attacked by the F^- ion forming a C–F bond, which would be an extremely high-energy process because of electrostatic repulsions. Strong similarities between absorption spectra of the pink solution of **1** produced by excess F^- (Figure 3c) and electrochemically generated NDI^{2-} at -900 mV vs Ag/AgCl, DMF in the absence of F^- (Figure 3d, SEC, pink trace) strongly support the first scenario. A higher relative intensity of the 542 nm band of the F^- -induced quickly generated pink solution than that of slowly (diffusion controlled) electrochemically reduced NDI^{2-} may be attributed to degradation of reduced NDI species under the UV/Vis light during prolonged SEC experiments. Consistent with the formation of NDI^{2-} by excess F^- , the pink solution of **1** became EPR silent (SI, Figure S4).

The presence of the $[\mathbf{1}\cdot\text{F}^-]$ complex at ≤ 1 equiv of F^- suggests that NDI^- may exist in the electron delocalized $\text{NDI}/\text{F}^- \leftrightarrow \text{NDI}^-/\text{F}^-$ anion– π and CT complex. In contrast, ESI-MS in the presence of excess F^- reveals only the $[\mathbf{1}]^{2-}$ dianion at m/z 210.40 but does not show any signal representing $[\mathbf{1}/\text{F}_n]^{n-}$ ($n \geq 1$) complexes (SI, Figure S2c). Therefore, only the first $F^- \rightarrow \text{NDI}$ ET event that produces NDI^- is facilitated by NDI/F^- anion– π binding, whereas the formation of NDI^{2-} with an additional F^- ion takes place through the direct chemical reduction of NDI^- and not via a physical binding of F^- with NDI^- due to electrostatic repulsions (Figure 1a). ESI-MS also confirms that once the NDI^{2-} dianion is formed it does not associate with F^- anymore.

Oxidation of orange ($\mathbf{1}^-$) and pink ($\mathbf{1}^{2-}$) solutions with NOBF_4 decolorized them. Because of strong absorptions of NOBF_4 in 350–400 nm regions, regeneration of **1** could not be confirmed by UV/Vis spectroscopy. However, ^1H NMR spectroscopy confirmed complete recovery of **1** after NOBF_4 oxidation (*vide infra*). The reversibility of NDI/F^- interactions further proves that these are noncovalent interactions.

Preorganized NDI receptor **SR** displayed (SI, Figure S5a) similar two-step spectroscopic changes with F^- . In addition to binding a F^- ion between two terminal NDI units, forming an $\text{NDI}/\text{F}^-/\text{NDI}$ sandwich complex, **SR** and **LR** can potentially bind a second F^- ion in the amide cavities via H-bonding interaction (Figure 1b).

This interaction, however, did not produce an additional optical signal. NDI-free **CR** showed (SI, Figure S5b) a modest change in the UV region owing to $\text{NH}\cdots\text{F}^-$ interaction and possible deprotonation of amide protons.

Interestingly, NDI receptors did not show any significant spectroscopic change with other anions (SI, Figure S5c), although the $[\mathbf{1}\cdot\text{Cl}^-]$ complex was found in ESI-MS (m/z 455.07).³ To investigate the selectivity and sensitivity of **SR** toward F^- , it was titrated with F^- in the presence of 30 equiv of Cl^- (Figure 3e). While **SR** did not optically respond to Cl^- , it showed the characteristic two-step color change with F^- even in the presence of Cl^- , demonstrating the desired selectivity for the F^- ion. The selective colorimetric response of NDI receptors for F^- recognition compared to nonchromogenic binding of more polarized anions may be attributed to the smaller ionic radius (1.33 Å) and 2p orbital of the F^- ion.^{1d} These factors allow F^- to come into closer proximity of the NDI π -surface and engage in efficient anion- π and CT interactions through better orbital interactions with NDI π^* -orbitals.^{2b} Such interactions facilitate an electron transfer from F^- to the NDI π -system that produces the orange $\text{NDI}^{\cdot-}$ radical anion. Larger size, orbital mismatch,^{1d,2b} and weaker binding of Cl^- and other anions^{3b} with NDI π -systems could rationalize why they do not induce visible color change.

Effects of preorganization on the sensitivity of NDI receptors were probed by monitoring the F^- -induced fluorescence changes at the minimum receptor concentrations. The titration of **SR** (1 nM in DMSO) with F^- (30 nM), probed by 381 nm excitation, displayed a 4.5-fold amplification of the original 430 nm emission peak of the NDI unit and a 20-fold amplification of a new peak at 465 nm (Figure 3f). NDI **1** (10 μM in DMSO) showed a similar fluorescence profile and 5.5-fold increase of the 465 nm emission peak (Figure 3f, inset), albeit at 10^4 times higher concentrations than **SR**. The excellent nM sensitivity of **SR** vs weaker μM sensitivity of **1** supports our hypothesis that preorganization of two NDI units should improve the F^- affinity and sensitivity through stronger NDI/ F^- interactions. The high F^- ion sensitivity of preorganized receptors (**PR**) bode well for their potential applications as F^- ion sensors.

^1H and ^{19}F NMR titration experiments were conducted to gain a better insight into NDI/ F^- interaction (Figure 4). The ^1H NMR spectrum of receptor **1** reveals a singlet at 8.75 ppm corresponding to four identical NDI core protons (H_a) and two doublets at 7.58 and 8.81 ppm corresponding to H_b and H_c of the pyridine ring, respectively (Figure 4a). During the titration of **1** with F^- all signals became broad but none shifted at all, virtually ruling out the possibility of a $\text{CH}\cdots\text{F}^-$ H-bond formation. Consistent with UV/Vis results, only the H_a signal gradually disappeared as F^- reached 1 equiv, indicating the formation of the $\text{NDI}^{\cdot-}$ radical anion. The EPR spectrum of this species (SI, Figure S4) confirmed the presence of the $\text{NDI}^{\cdot-}$ radical anion. NOBF_4 oxidation of the $\mathbf{1}^{\cdot-}$ radical anion completely regenerated **1**, as the original NMR spectrum reappeared, showing the H_a signal at 8.75 ppm (SI, Figure S6). The fact that the H_a signal never splits as a result of NDI/ F^- interactions, a sign that would have indicated a loss of symmetry of the NDI core had a covalent C-F bond formed, rule out this possibility. These results support our hypothesis that NDI/ F^- interactions facilitate the $\text{F}^- \rightarrow \text{NDI}$ ET event that generates the $\text{NDI}^{\cdot-}$ radical anion (Figure 1a).

In **SR**, NDI core protons (H_A) and the bisamide linker (H_X) appeared at 8.73 and 11.25 ppm, respectively (Figure 4b). During the titration of **SR** with F^- the H_A signal gradually disappeared as the F^- ion concentration reached 1 equiv, while the H_X signal shifted slightly downfield, indicating that at first F^- binds with NDI units.

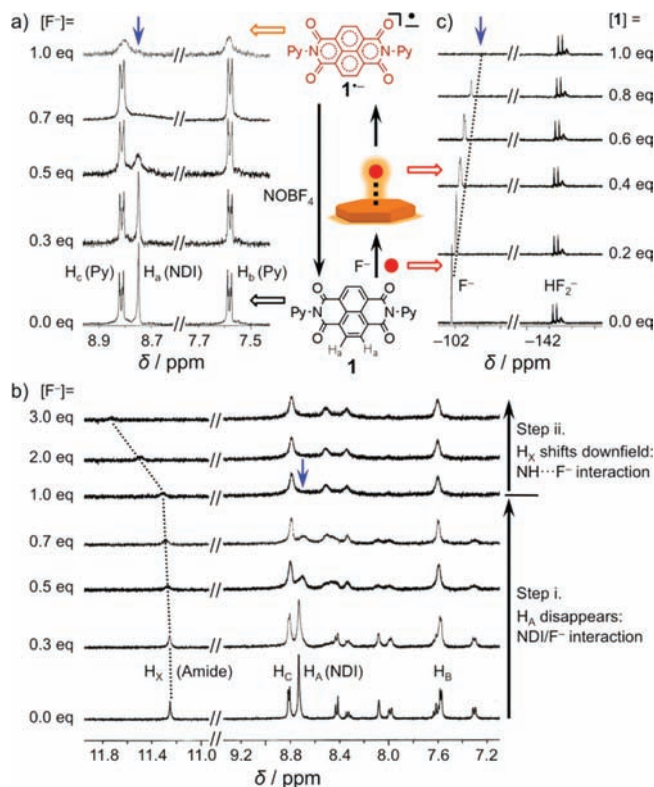


Figure 4. ^1H NMR titration of (a) **1** and (b) **SR** with F^- , and (c) ^{19}F NMR titration of **1** with F^- showing NDI/ F^- interaction (DMSO- d_6 , 298 K). Blue arrows: signal disappearance; dotted lines: signal shift.

NDI core protons in **SR** (Figure 4b) and **LR** (SI, Figure S7a) did not split before disappearing, potentially indicating the formation of NDI/ F^- /NDI sandwich complexes in which both NDI units interact evenly with the F^- ion. A significant downfield shift of the H_X signal at 1–2 equiv of F^- indicates subsequent $\text{NH}\cdots\text{F}^-$ H-bonding interaction with amide protons. These NMR results are consistent with ESI-MS data. In addition to showing $[\mathbf{SR}\cdot\text{F}^-]$ and $[\mathbf{LR}\cdot\text{F}^-]$ complexes at ≤ 1 equiv of F^- , ESI-MS of **SR** and **LR** in the presence of 2 equiv of F^- revealed signals that represent $[\mathbf{SR}\cdot 2\text{F}^-]$ and $[\mathbf{LR}\cdot 2\text{F}^-]$ complexes, respectively (SI, Figure S2d–g). These results confirm that **PRs** can bind up to two F^- ions. The binding of two F^- ions within one receptor molecule possessing two recognition sites has been reported previously.^{10a}

Thus, ^1H NMR titrations of **SR** and **LR** showing the disappearance of NDI signals before the onset of significant downfield shifts of amide signals, as well as ESI-MS showing the presence of $[\mathbf{PR}\cdot 2\text{F}^-]$ species, suggest that the first F^- ion binds through NDI/ F^- /NDI interaction and then a second F^- binds within the amide cavities (Figure 1b). The first \mathbf{PR}/F^- interaction is fully reversible by NOBF_4 oxidation (SI, Figure S6b), indicating that it involves NDI/ F^- interaction. In the presence of excess F^- , amide protons may be deprotonated, as their NMR signals became broad and finally disappeared and NDI units were further reduced to NDI^{2-} as the solutions turned pink. No F^- ion should be bound with the receptors at this stage because of strong electrostatic repulsions.

^1H NMR titrations of receptor **1** with Cl^- and other anions did not display any change (SI, Figure S8a), confirming that NDI/ Cl^- anion- π interaction is weak.^{3b} It can be attributed to weaker electronic interactions of the NDI unit with larger anions compared to a stronger electronic interaction with F^- . Titrations of receptor **1**, **SR**, and **LR** with Cl^- , Br^- , and I^- did not affect NDI protons. Only the ^1H NMR signals of amide protons in **SR** and **LR** shifted

downfield in the presence of Cl^- , showing that Cl^- preferentially binds inside the cavities of amide linkers via stronger $\text{N}-\text{H}\cdots\text{Cl}^-$ H-bonding interaction (SI, Figure S8b–c).

Fluoride ion recognition by NDI receptors was also observed from ^{19}F NMR spectroscopy. The ^{19}F NMR spectrum of $\text{TBAF}\cdot 3\text{H}_2\text{O}$ in $\text{DMSO}-d_6$ shows (Figure 4c) a strong singlet at -102 ppm corresponding to the F^- ion and a weak doublet at -142.5 ppm for HF_2^- .¹² Titrations of TBAF with **1** caused an upfield shift of the -102 ppm signal (Figure 4c), which indicates shielding of F^- by the NDI receptor. The disappearance of the F^- signal at 1:1 TBAF/**1** may be attributed to an oxidation of F^- to F^\bullet as a result of the $\text{F}^- \rightarrow \text{NDI}$ ET process that produces the $\text{NDI}^{\bullet-}$ radical anion. Although we previously considered a possibility of C–F bond formation as one of the modes of NDI/F^- interaction, it was not supported by any evidence, including ^{19}F NMR, as no new signal corresponding to a covalent C–F bond was observed.

The fact that F^- induced reductions of NDI to $\text{NDI}^{\bullet-}$ and NDI^{2-} can be fully reversed by oxidizing them back to neutral NDI with NOBF_4 and that the process can be repeated (SI, Figure S6a) confirm that F^- or the resulting F^\bullet never reacts with any NDI species covalently. Whether the transient F^\bullet reacts ultimately with solvent molecules, TBA counterions, homocouples to emanate F_2 gas, or generates HF acid remains unclear after extensive analyses of NDI/F^- mixtures. Nevertheless, F^\bullet is produced as a result of NDI/F^- interaction and ET events. Therefore, the lack of precise information on the fate of F^\bullet is inconsequential, as it does not impede the clear understanding of NDI/F^- anion– π interaction that leads to an unprecedented $\text{F}^- \rightarrow \text{NDI}$ ET event.

To demonstrate a potential application of NDI/F^- interaction, **SR** was treated individually with aqueous DMSO extracts of an anticavity toothpaste containing 0.24% (w/v) NaF and F^- -free toothpaste. To our delight, colorless **SR** turned light orange and displayed the absorption spectrum of the $\text{NDI}^{\bullet-}$ radical anion with the F^- containing toothpaste but did not show any optical changes with the F^- -free one (SI, Figure S9).

For the first time, a strong NDI/F^- interaction was identified and fully characterized by experimental results, as well as validated by computational models (SI, B3LYP/6-31+G**). Supramolecular NDI/F^- (anion– π and CT) interactions promote an unprecedented electron transfer process from the F^- ion to electron deficient NDI receptors. NDI receptors are highly selective toward F^- over other anions because of better orbital interactions. They display nM range F^- sensitivity in preorganized systems, in which two NDI units perfectly overlap with each other. The reversibility of the colorimetric response and reproducibility of NDI receptors render them excellent reusable F^- ion sensors. Therefore, NDI derivatives may

be exploited for the detection of various levels of F^- ion concentrations in drinking water, consumer products, as well as bone and muscle tissues for the early detection and prevention of F^- ion related diseases.

Acknowledgment. S.S. thanks FSU for financial support and Profs. Naresh Dalal and Igor Alabugin for assistance with EPR studies and B3LYP/6-31+G** calculations, respectively.

Supporting Information Available: Energy minimized structures; synthesis and characterizations; additional NMR, EPR, SEC, and ESI-MS data. This material is available free of charge via the Internet at <http://pubs.acs.org>.

References

- (1) (a) Quiñero, D.; Garau, C.; Rotger, C.; Frontera, A.; Ballester, P.; Costa, A.; Deyà, P. M. *Angew. Chem., Int. Ed.* **2002**, *41*, 3389–3392. (b) Alkorta, I.; Rozas, I.; Elguero, J. *J. Am. Chem. Soc.* **2002**, *124*, 8593–8598. (c) Rosokha, Y. S.; Lindeman, S. V.; Rosokha, S. V.; Kochi, J. K. *Angew. Chem., Int. Ed.* **2004**, *43*, 4650–4652. (d) Mascá, M. *Angew. Chem., Int. Ed.* **2006**, *45*, 2890–2893. (e) Mascá, M.; Yakovlev, I.; Nikitin, E. B.; Fetting, J. C. *Angew. Chem., Int. Ed.* **2007**, *46*, 8782–8784. (f) Hay, B. P.; Bryantsev, V. S. *Chem. Commun.* **2008**, 2417–2428. (g) Schottel, B. L.; Chifotides, H. T.; Dunbar, K. R. *Chem. Soc. Rev.* **2008**, *37*, 68–83. (h) Berryman, O. B.; Johnson, D. W. *Chem. Commun.* **2009**, 3143–3153. (i) Arranz, P.; Bianchi, A.; Cuesta, R.; Giorgi, C.; Godino, M. L.; Gutiérrez, M. D.; López, R.; Santiago, A. *Inorg. Chem.* **2010**, *49*, 9321–9332.
- (2) (a) Yoo, J.; Kim, M.-S.; Hong, S.-J.; Sessler, J. L.; Lee, C.-H. *J. Org. Chem.* **2009**, *74*, 1065–1069. (b) Chifotides, H. T.; Schottel, B. L.; Dunbar, K. R. *Angew. Chem., Int. Ed.* **2010**, *49*, 7202–7207.
- (3) (a) Gorteau, V.; Bollot, G.; Mareda, J.; Perez-Velasco, A.; Matile, S. *J. Am. Chem. Soc.* **2006**, *128*, 14788–14789. (b) Dawson, R. E.; Henning, A.; Weimann, D. P.; Emery, D.; Ravikumar, V.; Montenegro, J.; Takeuchi, T.; Gabutti, S.; Mayor, M.; Mareda, J.; Schalley, C. A.; Matile, S. *Nat. Chem.* **2010**, *2*, 533–538.
- (4) (a) Beer, P. D.; Gale, P. A. *Angew. Chem., Int. Ed.* **2001**, *40*, 486–516. (b) Caltagirone, C.; Gale, P. A. *Chem. Soc. Rev.* **2009**, *38*, 520–563.
- (5) (a) Lokey, R. S.; Iverson, B. L. *Nature* **1995**, *375*, 303–305. (b) Andric, G.; Boas, J. F.; Bond, A. M.; Fallon, G. D.; Ghiggino, K. P.; Hogan, C. F.; Hutchison, J. A.; Lee, M. A. -P.; Langford, S. J.; Pilbrow, J. R.; Troup, G. J.; Woodward, C. P. *Aust. J. Chem.* **2004**, *57*, 1011–1019.
- (6) Kirk, K. L. *Biochemistry of the Halogens and Inorganic Halides*; Plenum: New York, 1991; p 58.
- (7) (a) Ayoob, S.; Gupta, A. K. *Crit. Rev. Environ. Sci. Technol.* **2006**, *36*, 433–487. (b) Bassin, E. B.; Wypij, D.; Davis, R. B.; Mittleman, M. A. *Cancer Causes and Control* **2006**, *17*, 421–428.
- (8) Kauffman, J. M. *J. Am. Phys. Surg.* **2005**, *10*, 38–44.
- (9) (a) Wade, C. R.; Broomsgrrove, A. E. J.; Aldridge, S.; Gabbai, F. P. *Chem. Rev.* **2010**, *110*, 3958–3984. (b) Zhao, H.; Gabbai, F. P. *Nat. Chem.* **2010**, *2*, 984–990. (c) Tripier, R.; Platas-Iglesias, C.; Boos, A.; Morfin, J.-F.; Charbonnière, L. *Eur. J. Inorg. Chem.* **2010**, 2735–2745.
- (10) (a) Takeuchi, M.; Shioya, T.; Swager, T. M. *Angew. Chem., Int. Ed.* **2001**, *40*, 3372–3376. (b) Kang, S. O.; Llinares, J. M.; Powell, D.; VanderVelde, D.; Bowman-James, K. *J. Am. Chem. Soc.* **2003**, *125*, 10152–10153. (c) Bhosale, S. V.; Bhosale, S. V.; Kalyankar, M. B.; Langford, S. J. *Org. Lett.* **2009**, *11*, 5418–5421. (d) Gale, P. A. *Chem. Commun.* **2008**, 4525–4540. (e) Cametti, M.; Rissanen, K. *Chem. Commun.* **2009**, 2809–2829.
- (11) Hamuro, Y.; Geib, S. J.; Hamilton, A. D. *J. Am. Chem. Soc.* **1997**, *119*, 10587–10593.
- (12) Sun, H.; DiMugno, S. G. *J. Am. Chem. Soc.* **2005**, *127*, 2050–2051.

JA107382X